Boosting mass spectrometry-based analytics for biopharma

Gstöttner, C.J.

Chapter 6

Intact and subunit-specific analysis of bispecific antibodies by sheathless CE-MS

Christoph Gstöttner[a], Simone Nicolardi[a], Markus Haberger[b], Dietmar Reusch[b], Manfred Wuhrer[a], Elena Domínguez-Vega[a]

[a]Leiden University Medical Center, Center for Proteomics and Metabolomics, Leiden, The Netherlands

[b]Roche Pharma Technical Development, Penzberg, Germany

Reprinted and adapted with permission from Anlytica Chimica Acta, 2020, 1134, 18-27, DOI: 10.1016/j.aca.2020.07.069

6.1 Abstract

Bispecific antibodies (BsAb) are next-generation, antibody-based pharmaceuticals which come with a great functional versatility and often a vast structural heterogeneity. Although engineering of the primary sequence of BsAbs guides the proper pairing of the different chains, several side products can often be observed contributing to the macroheterogeneity of these products. Furthermore, changes in the amino acid sequence can result in different protein modifications which can affect the properties of the antibody and further increase the structural complexity. A multi-methods approach can be used for the characterization of their heterogeneity but new analytical strategies are needed for a more accurate and in-depth analysis.

Here, we present a combination of intact antibody and subunit-specific mass measurements using sheathless capillary electrophoresis-mass spectrometry for assessing the macro- and microheterogeneity of BsAbs. Two homologous BsAbs with the same bispecificity but slightly different amino acid sequences were analyzed. Intact measurements were performed using a positively coated capillary and a background electrolyte (BGE) consisting of 3% acetic acid. For intact BsAbs, the separation permitted the characterization of free light chains, homo- and heterodimers as well as incomplete assemblies. For subunit-specific measurements, BsAbs were hinge region cleaved using two different enzymes (SpeB and IdeS) followed by disulfide-bond reduction. The six different subunits (Lc1, Lc2, Fd'1, Fd'2, (Fc/2)1 and (Fc/2)2) were separated using the same positively-coated capillary and a BGE consisting of 20% acetic acid and 10% methanol. Mass measurements of hinge region cleaved antibodies were performed at isotopic resolution (resolving power 140000 at m/z 1100) for a more confident analysis of low abundance proteoforms. For both BsAbs several proteoforms with e.g. pyroglutamic acid (Pyro-Glu) or glycation which could not be properly assigned at the intact level, were accurately determined in the subunits showing the complementarity of both approaches.

6.2 Introduction

The last decade has been marked by biotechnological innovations that have permitted the exploitation of novel ways of antibody production and biopharmaceuticals development. Traditional monoclonal antibodies (mAbs) are being slowly displaced by increasingly complex antibody formats which can tackle some limitations of mAbs (e.g. higher binding avidity, lower resistance or higher cytotoxicity[1]) opening new ways for therapeutic intervention[2]. Examples of these formats are Fc-fusion proteins[3] or bispecific monoclonal antibodies (BsAbs)[4]. BsAbs, in particular, are taking a predominant position in biopharma as they can bind to two different epitopes. This makes BsAbs especially attractive for cancer immunotherapy as they can bring two target cells in close proximity (e.g. a cancer cell and a cytotoxic T cell). Another example is the treatment of haemophilia A by the recently approved BsAb emicizumab which binds the blood coagulation factors IX and X[5].

Production of bispecific antibodies requires proper assembly of two different light chains (Lc) and two different heavy chains (Hc). Recent strategies in antibody engineering such as knob-into-hole (for Hc-Hc pairing) or crossmab (for Lc-Hc assembly) have enabled efficient pairing of chains within BsAbs (**Figure 1A**)[6, 7]. Still, side products such as free chains, incomplete antibodies or aggregates are commonly observed during production which can induce unwanted immunological responses[8]. This so-called macroheterogeneity should be carefully monitored to ensure patient safety. In addition, antibodies are inherently heterogeneous molecules containing different glycoforms and many other post-translational modifications (PTMs) which can impact the functionality of the antibody[9, 10]. Importantly, the location of these modifications can influence their effect on the functionality of the protein. For instance, oxidation will affect antigen binding or reduce the half-life of the antibody depending on whether it is positioned in the antigen binding fragment (Fab) or in the Fc region[10, 11]. Therefore, next to the identification also the assignment to antibody domains is important.

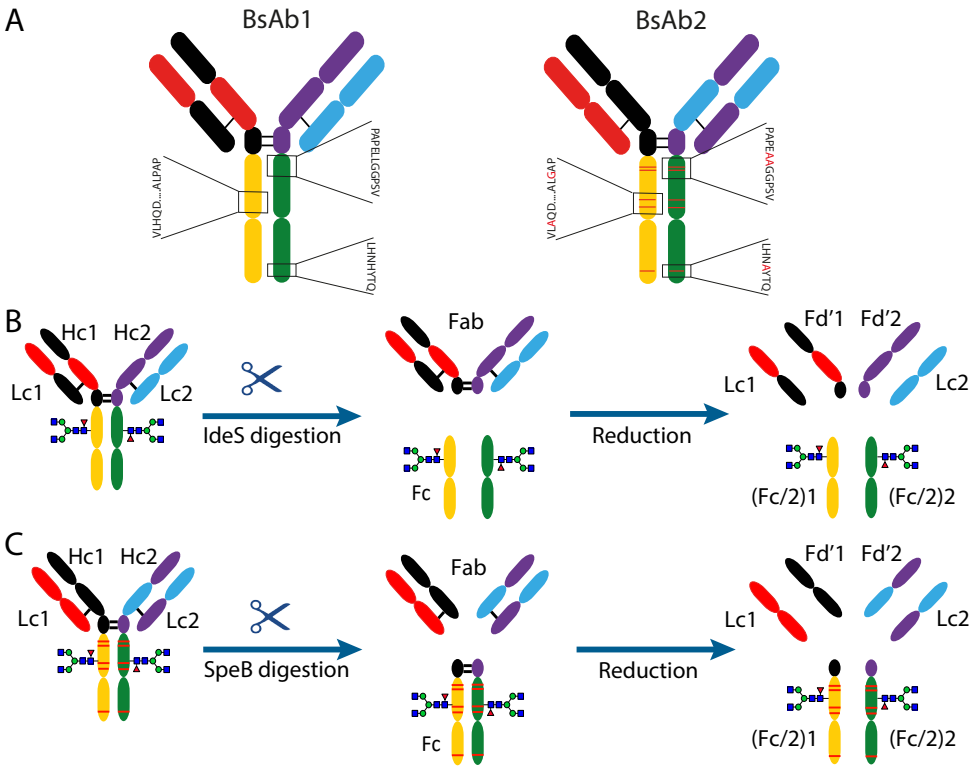

Figure 1. A) Comparison of amino acid differences between BsAb1 and BsAb2. Exchanged amino acids are shown in red. Glycans are removed for simplicity. Hinge region cleavage and reduction of BsAbs leading to six different subunits. B) IdeS digestion and reduction of BsAb1. C) SpeB cleavage and reduction of BsAb2. Red stripes in the Fc indicate LALA PG mutation. (For interpretation of the references to color in this figure legend, the reader is referred to the Web version of this article.)

Mass spectrometry (MS) has become the core technique for structural characterization of mAbs. For the characterization of the microheterogeneity of conventional mAbs several bottom-up approaches (*i.e.* after enzymatic digestion) have been described[12]. These approaches provide essential information on the sites that are modified but do not allow conclusions on the assembly of antibodies or co-occurrence of modifications. Intact protein analysis approaches are increasingly being used for mAb characterization[12-16] as they provide a clear overview of the macroheterogeneity and, to a certain extent, microheterogeneity (*e.g.* glycosylation) of the sample. However, they fail to resolve isomeric proteoforms as well as modifications with only small mass differences (e.g. deamidation, glycation vs glycosylation) and do not localize the modification within different domains. Over the last years, analysis of individual subunits (i.e. after hinge region cleavage and disulfide bridge reduction) is becoming an indispensable part of intact antibody characterization[17]. This allows decreasing the complexity of the molecule (mass of subunits ~25 kDa) adding

confidence to the assignment of low mass differences, but also allocating the modifications to domains and subunits. The combination of intact antibody and subunit analysis provides a reliable assessment of both macro- and microheterogeneity. However, due to the large differences in mass their analysis often required different analytical strategies. For the macroheterogeneity analysis, SEC-MS is generally used[13],[18-20] while for subunit analysis RPLC-MS[21-23] or HILIC-MS[24] are more suitable.

Capillary electrophoresis (CE)-MS has demonstrated to be a powerful technique to analyze intact proteins and their proteoforms. Due to the characteristics of the separation capillary (open tube), CE can be used to separate proteins of a wide range of sizes. This makes CE-MS a very attractive technique for the analysis of both, intact mAbs and subunits without the need for alternative platforms[25-28]. In particular, when hyphenated via the sheathless interface, high ionization efficiencies and sensitivity can be obtained which might be especially useful for the detection of low abundant PTMs. Sheathless CE-MS has already demonstrated its ability to separate either intact[27] or hinge region-cleaved[25, 26, 29] monospecific mAbs and their proteoforms. BsAbs, however, present larger macroheterogeneity due to the more complex production process. Furthermore, after hinge region cleavage and reduction, engineered BsAbs consist generally of six individual subunits (**Figure 1B and C**) instead of the three commonly present in traditional mAbs. Therefore, in this work, we explore the use of sheathless CE-MS for intact and subunit-specific characterization of BsAbs. Two homologous BsAbs obtained by different engineering processes were included in the study. Analysis of the intact BsAbs allowed monitoring incomplete assemblies and free chains. Using two alternative hinge region-specific enzymes, the six individual subunits were obtained and consequently characterized using sheathless CE-MS. This permitted the determination of PTMs such as glycation and assignment to specific portions of the molecule.

6.3 Materials and Methods

6.3.1 Reagents

Sodium hydroxide (≥99.8%), di-thiothreitol (DTT) (≥98%), tris(2-carboxyethyl)phosphine (TCEP) (≥98%), hydrogen chloride (ACR reagent grade 37%), sodium chloride (≥99.8%), methanol anhydrous (≥99.8%) and Tris-HCl (≥99.8%) were obtained from Sigma-Aldrich (St. Louis, MO). Methanol (Ultra LC-MS grade) was provided by Actu-All Chemicals (Randmeer, Oss, The Netherlands). Water (ULC/MS - CC/SFC grade) was purchased from Biosolve Chimie SARL (Dieuze, France). $NaHCO_3$ (≥99.7%), was purchased from Merck KGaA (Darmstadt, Germany). Acetic acid (≥99.7%) was purchased from VWR Chemicals (Radnor, PA). 8 M aqueous solution Guanidinium chloride (GdnCl) was obtained from Thermo Scientific (Waltham, MA). Ammonium acetate stock solution 7.5 M (for molecular biology) was purchased from Sigma-Aldrich. 50% tri-methoxysilylpropyl modified polyethylenimine (PEI) solution in isopropanol was obtained from Gelest (Morrisville, NC). IdeS (Fabricator) and

SpeB (Fabulous) endoproteinases were purchased from Genovis (Lund, Sweden). Formulated BsAb1 (pI 7.6) and BsAb2 (pI 7.4) were provided by Roche Diagnostics (Penzberg, Germany). The protein test mixture was obtained from Sciex (Brea, CA).

6.3.2 Sample preparation for intact BsAbs measurement

For intact measurements, BsAb1 and BsAb2 were three times desalted with water using 10 kDa Vivaspin MWCO filter tubes (Sartorius, Göttingen, Germany) at 10000xg at 4 °C. The samples were afterward diluted to a final concentration of 1 µg/µL and either directly measured or stored for a short period at 4 °C.

6.3.3 Hinge region cleavage of BsAbs

Two enzymes were used for the hinge region cleavage of the bispecific antibodies (IdeS and SpeB for BsAb1 and BsAb2, respectively). For IdeS digestion, the BsAb1 was diluted in 100 mM $NaHCO_3$ pH 6.8 (adjusted with acetic acid) to a final concentration of 1 µg/µL. For digestion, one Unit of IdeS per µg of mAb was added and incubated for 90 min at 37 °C. For SpeB digestion, the BsAb2 was diluted in 100 mM Tris-HCl pH 8.0 to a final concentration of 1 µg/µL and incubated with SpeB (one unit per µg mAb) at 37 °C for 60 min.

6.3.4 Reduction of hinge region cleaved BsAbs

After hinge region cleavage, BsAbs were denatured by diluting the BsAbs 1:1 (v:v) with 8 M GdnCl in 100 mM Tris pH 8.0 solution. After dilution, 1 M DTT was added to a final concentration of 20 mM. The samples were incubated at 60 °C for 30 min. After reduction, the samples were three times desalted with either water (BsAb1) or 100 mM ammonium acetate pH 3.0 (BsAb2) using 10 kDa Vivaspin MWCO filter tubes at 10000x*g* at 4 °C. The samples were directly measured or stored for a short period at 4 °C.

For TCEP reduction, used during reduction optimization, a 1 M TCEP solution in 100 mM $NaHCO_3$ at pH 6.8 was prepared and added to the sample to a final concentration of 100 mM TCEP. Samples were desalted as described above.

6.3.5 Sheathless CE-MS

Sheathless CE-MS experiments were performed on a Sciex CESI 8000 instrument. Bare fused silica capillaries with a porous tip were obtained from Sciex (separation capillary: 91 cm x 30 µm i.d, capillary volume 643 nL; conductive line: 70 cm x 50 µm i.d., capillary volume 1374 nL) and were in-house coated with PEI following the protocol described by Sciex[30]. Briefly, the capillaries were pre-conditioned by flushing the separation capillary for 20 min with 0.1 M NaOH (75 psi, forward pressure, 21 capillary volumes), 10 min (75 psi, forward pressure, 10.5 capillary volumes) with 0.1 M HCl, 20 min with H_2O (75 psi, forward pressure, 21 capillary volumes), 20 min with MeOH (75 psi, forward pressure, 21 capillary

volumes) and the conductive line 5 min with MeOH (50 psi, reverse pressure). Subsequently, the separation capillary was flushed with PEI coating solution for 30 min (75 psi, forward pressure, 31.5 capillary volumes) and incubated overnight. The next day the capillary was cleaned with MeOH for 10 min (75 psi, forward pressure, 10.5 capillary volumes), 30 min from a second vial with MeOH (75 psi, forward pressure 31.5 capillary volumes) and 5 min the conductive line with MeOH (100 psi, reverse pressure). Hereafter, the separation capillary was conditioned by flushing it for 3 min with H_2O (100 psi, forward pressure, 4.2 capillary volumes), 2 min with 1 M NaCl (100 psi, forward pressure, 2.8 capillary volumes), followed by 3 min with H_2O (100 psi, forward pressure 4.2 capillary volumes) and the conductive line for 3 min with H_2O (100 psi, reverse pressure). For the performance check the separation capillary and conductive line were filled with 100 mM ammonium acetate pH 3.0 (8 min at 100 psi forward pressure, 11.2 capillary volumes, and 4 min at 100 psi reverse pressure). The performance of the capillary was checked using the protein test mixture. Intact measurements were performed using a BGE of 3% acetic acid. For hinge region cleaved BsAbs 20% acetic acid containing 10% methanol was used as BGE. Before each run, the separation capillary was flushed for 4 min with BGE (100 psi, forward pressure, 4.2 capillary volumes) and the conductive line for 2 min with BGE (75 psi, reverse pressure). The samples were injected by applying 2.5 psi for 15 s (5.6 nL, 0.87% of the total capillary volume) followed by a plug of BGE (0.5 psi for 25 s, 1.9 nL). The separations were performed at 20 °C by applying 20 kV at reversed polarity for 45 min. After each run, the capillary was ramped down to 1 kV in 5 min.

The capillary, containing a grounded sheath metal, was connected via a nano-electrospray ionization source, which could be adjusted via a XYZ stage either to an Impact qTOF-MS or a solariX 12 T FT-ICR-MS equipped with a ParaCell (Bruker Daltonics, Bremen, Germany). The system operated in positive mode using a capillary voltage of 1200 V, a dry gas flow of 1.8 L/min and temperature of 180 °C. For the Qtof-MS, the quadrupole ion energy and collision cell voltage were set at 5.0 and 20.0 eV, respectively. Transfer and pre-pulse storage times were 120.0 and 25.0 µs, respectively. For in-source collision-induced dissociation (isCID) 100 eV between funnel 1 and 2, was used. The monitored *m/z* range was 500–6000. During FT-ICR-MS analysis the trapping potentials were set to 5.5 V and the ParaCell DC biases up to 1.5 V. The Q1 mass was set to *m/z* 800 while the time-of-flight to the ICR cell was set to 1.2 ms. The mass spectra were acquired in an *m/z*-range of either 202.70-3000, 405.41-3000 or 589.68-3000 with 1 M data points (with transient times either 0.144, 1.25 or 1.78 s). The accumulation time was 0.1 s. Mass spectra deconvolution was performed using the maximum entropy algorithm in the DataAnalysis software from Bruker Daltonics (Bremen, Germany). Monoisotopic masses were determined using the SNAP option from de DataAnalysis software after deconvolution.

6.4 Results and Discussion

We analyzed two antibodies, namely BsAb1 and BsAb2, with the same bi-specificity and affinity but slightly different amino acid sequences due to the different engineering approaches. BsAb1 has a CH1-CL exchange in the binding site 1, a knob-into-hole in the CH3 but no additional amino acid substitutions in the CH2 portion (**Figure 1A**). BsAb2 has a CH1-CL exchange in the binding site 2, a knob-into-hole in the CH3 (with an additional exchange of 2H for 2A in the CH2 and CH3 subunits) and an L250A L251A P345G mutation in the CH2 portion introduced to "silence" the interaction with FcRs (**Figure 1A**)[31].

6.4.1 Intact mass measurements of BsAbs

BsAbs consist of four different chains that need to be correctly assembled during production often resulting in larger macroheterogeneity than traditional mAbs. In this study, we aimed to explore the potential of sheathless CE-MS to monitor the proper assembly of BsAbs.

Sheathless CE-MS analysis of BsAbs was performed using a positive coated capillary to avoid adsorption of the positively-charged proteins to the capillary wall. PEI was selected as it provides stable covalently-bound positive surfaces with a pH-independent anodic electroosmotic flow. This allows us to obtain efficient protein separations and provides good nanospray stability without the need of additional pressure during separation. Different BGEs were evaluated for intact BsAbs separations (**Figure S1**). Using 25 mM acetic acid, the effect of the pH on the separation and detection of BsAbs and their assemblies was evaluated. Increasing the pH from 3.0 to 6.5 did not result in the detection of additional assemblies (i.e. non-covalent assemblies) while it had a negative influence on in the sensitivity due to the presence of ammonium ions which suppress the ionization. Therefore, analyses of intact BsAbs were performed at low pH. Increasing the concentration of acetic acid from 25 to 500 mM (3%) resulted in resolution of several peaks corresponding to different protein subunits and assemblies (**Figure 2A**). Good sensitivity and quality of the mass spectra were observed using these conditions (**Figure S2**). The assignments with the mass error of the different detected signals are shown in **Table 1**.

Table 1. Assignment of the species detected after sheathless CE-MS analysis of intact BsAb1.

Peak	Proteoform			Theoretical average mass (Da)	Observed average mass (Da)	Error (Da)
5		Lc1 Lc1 (+Cys) Lc1 (+GSH)		22172.4 22292.5 22478.7	22173.0 22291.9 22478.2	0.6 0.6 0.5
4		Lc2 Lc2 (+Cys) Lc2 (+GSH)		23445.8 23565.9 23752.1	23445.3 23565.1 23751.3	0.5 0.8 0.8
		Lc1-Lc2		45618.1	45617.6	0.5
		Lc2-Lc2		46891.5	46890.9	0.6
3	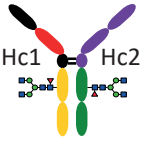	Hc1-Hc2	(G0F/G0)* (G0F/G0F) (G0F/G1F)* (G1F/G1F)# (G1F/G2F)* (G2F/G2F)	103742.1 103888.2 104050.4 104212.5 104374.7 104536.8	103747.7 103887.9 104054.1 104212.6 104377.2 104533.2	3.6 2.5 0.1 3.7 0.3 5.6
2	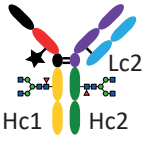	BsAb (-Lc1) (+Cys)	(G0F-G0)* (G0F-G0F) (G0F-G1F)*	127308.0 127454.2 127616.3	127307.8 127454.0 127621.6	0.2 0.1 5.3
		BsAb (-Lc1) (+GSH)	(G0F/G0F) (G0F-G1F)* (G1F-G1F)	127640.3 127802.5 127616.3	127638.0 127796.3 127960.9	2.3 6.2 3.7
	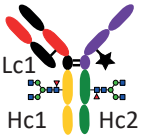	BsAb (-Lc2) (+Cys)	(G0F/G0)* (G0F/G0F)	126034.6 126180.7	126029.7 126176.5	4.9 4.2
		BsAb (-Lc2) (+GSH)	(G0F/G0F) (G1F/G0F)*	126366.9 126529.1	126365.2 126527.0	1.7 2.1

1	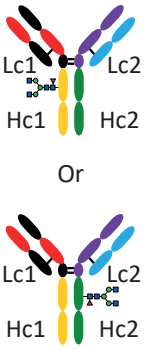	BsAb (singly glycosylated)	G0 G0F G1F G2F	147914.9 148061.0 148223.1 148385.3	147918.7 148062.3 148222.9 148388.0	3.9 1.3 0.3 2.7
	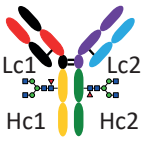	BsAb	(G0/G0) (G0F/G0)* (G0F/G0F) (G0F/G1F)* (G1F/G1F)# (G1F/G2F)* (G2F/G2F)	149214.1 149360.2 149506.3 149668.5 149830.6 149992.8 150154.9	149216.7 149361.2 149505.7 149666.6 149829.1 149992.1 150150.2	2.6 1.0 0.6 1.9 1.6 0.7 4.7

The main peak (peak 1) corresponded to the intact antibody with different glycoforms, ranging from G0/G0 to G2F/G2F (Inset **Figure 2A**). The intact antibody was detected with lysine clipping (Kclip) on both heavy chains as well as with a mass difference of ~36 Da lower which suggests two pyroglutamic acid formations either on Lc1 and Hc1 coming from glutamine or on Hc2 coming from glutamic acid. However, at the intact level, we could not assign which of these three chains were modified. In peak 1, a low abundance signal (below 2% compared to the main form) was observed which corresponded to the BsAb missing one glycosylation in one of the Hc. Migrating in front of the main peak (peak 2) we detected the BsAb missing either Lc1 or Lc2 and their corresponding glycoforms. In both cases, the cysteine of the non-paired Hc was observed cysteinylated (+120.2 Da) or glutathionylated (+306.3 Da). In peak 3 we observed the correctly assembled Hc dimer missing both Lcs (Mw ~ 100 kDa). The Hc dimer was preceded by two species of approximately 45 kDa which corresponded to the Lc hetero- (Lc1-Lc2) and homodimers (Lc2-Lc2) (peak 4). Finally, in peak 5 of the electropherogram, free Lc1 and Lc2 either non-modified, cysteinylated, or glutathionylated were observed. These results illustrate the larger macroheterogeneity of BsAbs compared to standard monospecific mAbs where fewer possibilities for misassembling such as heterodimers can occur.

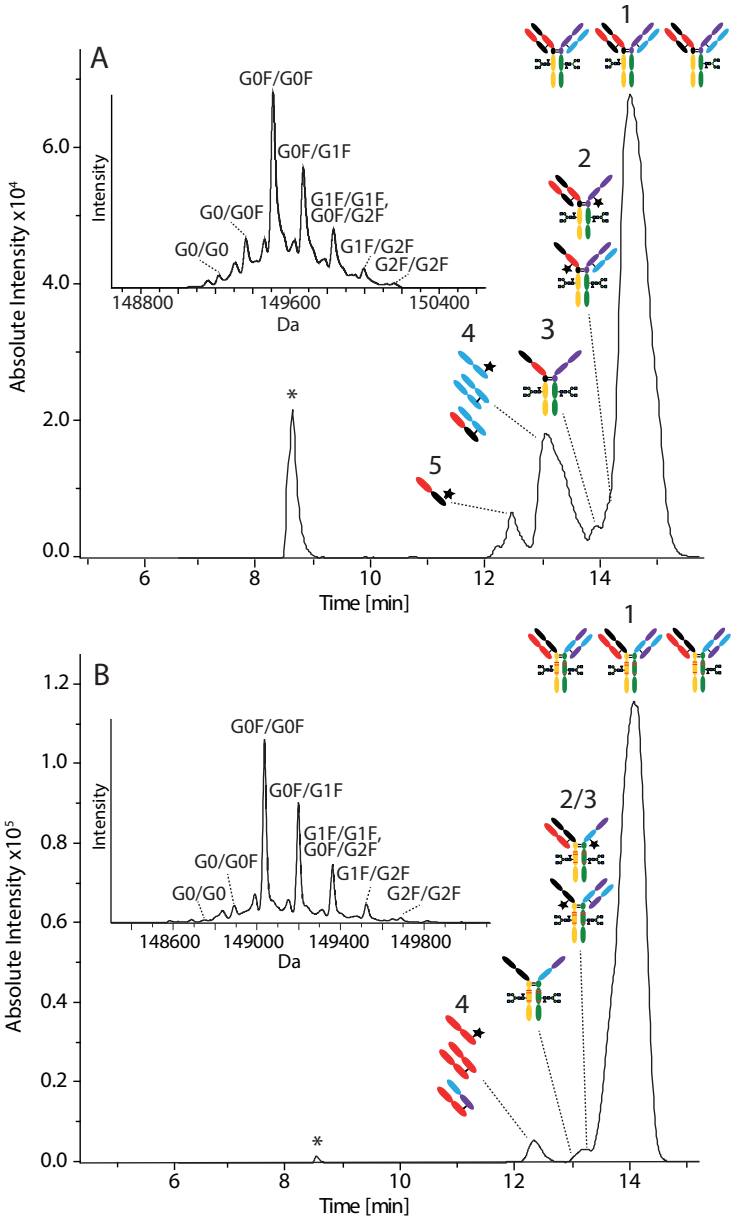

Figure 2. Sheathless CE-qTOF-MS of intact BsAbs. A) Base peak electropherogram (BPE) of BsAb1 (labeled from 1 to 5, see Table 1) and deconvoluted spectrum of peak 1 (inset). B) Base peak electropherogram (BPE) of BsAb2 (labeled from 1 to 4, see **Table S1**) and deconvoluted spectrum of peak 1 (inset). BGE: 10% Acetic acid. (*) non-protein peak.

Similar patterns were observed for the BsAb2 (**Figure 2B** and **Table S1**). The antibody was also detected with both C-terminal lysines clipped but only with one pyroglutamic

acid formation. In this case, the Lc1 does not contain terminal glutamine and, therefore, only the Hc1 and Hc2 can be modified. Regarding the different assemblies, although the antibody missing the crosslinked Lc (Lc2) was detected, no evidence was observed of free Lc2 in the MS. Also, the levels of Lc homo- and heterodimers observed for BsAb2 in peak 4 were lower compared to BsAb1. These results show that despite the large homology on the primary structure of these two antibodies, the different engineering processes resulted in an overall lower macroheterogeneity for BsAb2. Of note, for neither of the BsAbs evidence of mispairing (e.g. Hc1-Lc2) within chains was observed.

6.4.2 Hinge region digestion and reduction of differently engineered bispecific antibodies

Due to the presence of two binding sites and different engineering of the Fc region (knob-into-hole), BsAbs comprise six different subunits, namely Lc1 and Lc2, Fd'1 and Fd'2 and (Fc/2)1 and (Fc/2)2. These subunits, originally linked to form the typical Y-shape structure of immunoglobulin-G (IgG) mAbs, can be separated by proteolytic hinge region cleavage and reduction of disulfide bonds (**Figure 1B** and **C**). Compared to conventional IgG1-mAbs, the hinge region of BsAb1 is not altered. The enzyme IdeS exhibits a high specificity to cleave IgG1 antibodies just below the hinge region (PELLG/GPS in CH2 domain) and has been extensively used for subunit-specific characterization of conventional mAbs [26, 32-34]. Thus, IdeS was selected for the digestion of the BsAb1. Using IdeS no intact antibody was detected after a 90 min digestion indicating efficient proteolytic cleavage (Figure S3). BsAb2 contains an L250A L251A P345G mutation in the CH2 portion (**Figure 1A**). These amino acid substitutions are close to the cleavage site of the IdeS (PEAAG/GPS) hampering the cleavage of the antibody (no enzymatic cleavage achieved, data not shown). Therefore, a second enzyme, SpeB, was evaluated. In contrast to IdeS, SpeB cleaves above the hinge region (SCDKT/HPC) (**Figure 1C**) efficiently allowing the digestion of BsAb2. Using SpeB and digestion time of 60 min complete cleavage of BsAb2 was achieved (**Figure S3**).

After hinge region cleavage, the sample was reduced to generate the six individual subunits. eduction was performed using 100 mM TCEP or 20 mM DTT containing GdnCl as a chaotropic agent. Using TCEP the reduction of the BsAb subunits was not complete resulting in a complex mixture of different chains with different reduction levels. For Lc1 the reduced Lc1 (22164.18 Da) and the Lc1 with one internal disulfide bridge closed (22162.26 Da) were observed (theoretical mass of fully reduced Lc1 22163.90 Da) (**Figure S4**). (Fc/2)1 and (Fc/2)2 were detected either completely reduced or with one or two disulfide bridges closed while both Fds were completely reduced under these conditions. Using 20 mM DTT with 4M GdnCl as a chaotropic agent full reduction was achieved (**Figure 3**) and only completely reduced chains and their proteoforms were detected. Therefore 20 mM DTT with GdnCl was used to reduce the BsAbs after the hinge region cleavage.

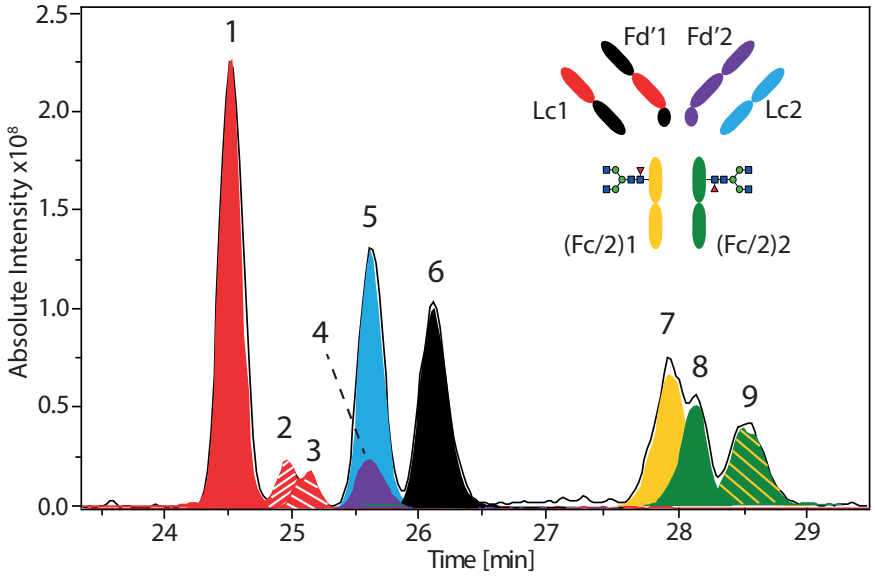

Figure 3. BPE (black trace) and EIEs (color fill) for the six chains and proteoforms of BsAb1 obtained by sheathless CE-FT-ICR-MS after IdeS cleavage and DTT reduction (labelled from 1-8, compare **Table 2**). Peak number 9 contains both Fc/2 fragments as a complex. BGE: 20% Acetic acid containing 10% MeOH. EIEs: Peak 1 (1009.10+1057.06+1109.96±0.1 m/z); Peak 2 (1009.78+1057.91+1110.70±0.1 m/z); Peak 3 (999.50+1047.14+1099.50±0.1 m/z); Peak 4 (1038.80+1082.04+1129.09±0.1 m/z); Peak 5 (1066.94+1117.75+1173.49±0.1 m/z); Peak 6 (1025.95+1065.41+1107.94±0.1 m/z); Peak 7 (927.83+963.49+1001.95±0.1 m/z); Peak 8 (938.26+974.26+1013.15±0.1 m/z); Peak 9 (1398.96+1438.98+1481.22±0.1 m/z).

6.4.3 BsAb subunit-specific characterization by sheathless CE-FT-ICR-MS

To address with high confidence the microheterogeneity of BsAbs a subunit-specific characterization is preferred. In this work, we also study the performance of sheathless CE-MS for the characterization of BsAb subunits. The separation of the subunits was performed applying the same PEI-coated capillary than for the intact mass measurements. For the separation of the subunits, different acidic BGEs were evaluated. Using 10% acetic acid most of the chains were separated, however, the comigration of some proteoforms was observed (**Figure S5**). The addition of an organic modifier increased the viscosity of the BGE and reduced the EOF often resulting in a better separation of proteins in positively-charged coated capillaries[25]. The addition of 10% MeOH to the BGE increased the separation window and allowed to resolve more species (**Figure S5**). A similar effect was observed with the increase of the acetic acid content from 10 to 20%, likely a consequence of the higher ionic strength. Further increase of acetic acid or MeOH content did not improve separation.

Using 20% acetic acid containing 10% MeOH all subunits were efficiently separated with the exception of Fd'2 and Lc2 which comigrated (**Figure 3**). These two subunits have very similar charge and hydrodynamic radius and, therefore, were not electrophoretically resolved (**Table S2**). For the rest of the subunits, although their hydrodynamic radius were very similar, their different number of charges allowed their CE separation (less positive proteins migrates earlier in positively-coated capillaries using reverse polarity) (**Table S2**). The formation of a Pyro-Glu on the N-termini of the Lc1 resulted in the loss of the primary amine and, therefore, in a lower electrophoretic mobility compared to the non-modified Lc. Glycosylation of the Fc/2, on the other hand, did not modify the charge of the protein and the different glycoforms comigrated in the same peak. Using 20% acetic acid containing 10% MeOH the repeatability of the method was assessed by the analysis of BsAb1 subunits after reduction and hinge-region digestion in three different days. The method showed good intraday (n=6) and interday (n=9) repeatability with RSD values of migration time between 0.5% and 1.7% (**Figure S6**).

Table 2. Assignment of the species detected by sheathless CE-MS for IdeS digested and reduced BsAb1.

Peak	Subunit	Sequence	PTM	Theoretical monoisotopic mass (Da)	Observed monoisotopic mass (Da)
1	Lc1	1-213	Pyro-Glu	22163.90	22164.04
2	Lc1	1-213	-	22180.92	22180.90
3	Lc1	3-213	truncation	21955.81	21955.79
4	Fd'2	1-242	-	25929.66	25930.01
5	Lc2	1-214	-	23436.43	23436.52
6	Fd'1	1-252	Pyro-Glu	27656.20	27656.37
7	(Fc/2)1	215-462 -Kclip	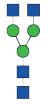	24862.32	24862.46
				25008.38	25008.51
			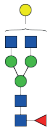	25170.43	25170.58
			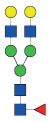	25332.49	25332.61

8	(Fc/2)2	243-452 -Kclip		25143.44	25143.56
				25289.50	25289.62
			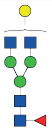	25451.55	25451.67
			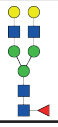	25613.61	25613.78
9	(Fc/2)1 + (Fc/2)2	215-462 -Kclip + 243-452 -Kclip	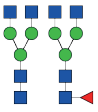	50151.82	50151.12
			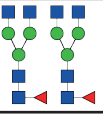	50297.88	50297.16
			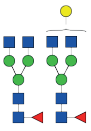	50460.93	50458.23
			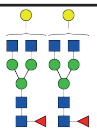 or 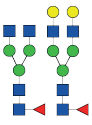	50621.98	50620.25

A complete subunit-specific characterization of the BsAb1 using the optimized conditions is presented in **Table 2**. To accurately assign all present proteoforms, we employed FT-ICR-MS. For the measurements, a transient time of 1.7476 s and a low *m/z* of 589.68 were used. **Figure S7** and **S8** show the 20+ charge state of Lc1 (*m/z* ~1110) with a resolving power of 145000. The used transient time permitted to isotopically resolve all the antibody subunits while providing enough spectra per peak. The intensity observed for the different subunits reflects their different ionization efficiency, with the Lc having the higher and the glycosylated Fc/2 portions the lower ionization efficiency. **Figure S9** shows the observed mass spectra for the six different subunits using CE-FR-ICR-MS, as well as the isotopic resolution obtained

for Lc1. This allowed the determination of their monoisotopic mass with an error between 2 and 13 ppm (**Table 2**). The deconvoluted mass spectra of all six subunits are shown in **Figure 4**. For both Fc/2 portions, several N-glycosylation forms (G0, G0F, G1F, and G2F) were observed being G0F the most abundant glycoform. In addition to glycosylation, other PTMs were detected within the BsAb1 subunits. Both Lc1 and Fd'1 were N-terminal pyroglutamic acid modified. Fd'2, which contains a terminal glutamic acid did not show this modification. For Lc1, both, unmodified and Pyro-Glu modified proteoforms could be detected while for Fd'1 only the Pyro-Glu form was observed. The middle-up analysis of BsAbs allowed the assignment of these modifications to each particular chain which was not possible at the intact level. However, due to the reduction step, the cysteinylated or glutathionylated free chains were not observed in the subunit-specific analysis. Peak 3 was assigned to the Lc1 with an N-terminal truncation (missing a proline and a glutamine). In addition to the different subunits and proteoforms, fragments with masses between 50151.12 and 50620.25 Da were observed (peak 9, **Figure 3**). These masses correlated well with the calculated mass for the two reduced Fc/2 subunits (Fc1/2+Fc2/2) (theoretical mass G0/G0F, 50151.82 Da; observed mass, 50151.12 Da). IdeS cleaves below the hinge region of the antibody and, therefore, these subunits may only be associated by non-covalent interactions. This type of associations has been previously described in CE-MS for IdeS-digested mAbs when acetic acid BGEs with concentrations below 10% were employed[26]. Higher concentrations or addition of organic solvents provided full dissociation of the Fc complex in the studied mAbs, resulting in only Fc/2 fragments in the electropherogram[26]. As mentioned earlier, the Fc portions of BsAb1 are modified (i.e. knob-into-hole) to ensure the correct assembly of the two different heavy chains. We hypothesize that the strong interaction between the introduced amino acids (knob-into-hole) kept part of the two engineered Fc/2 subunits together (or led to a fast reassembly) even in presence of BGEs with high acetic acid and MeOH content.

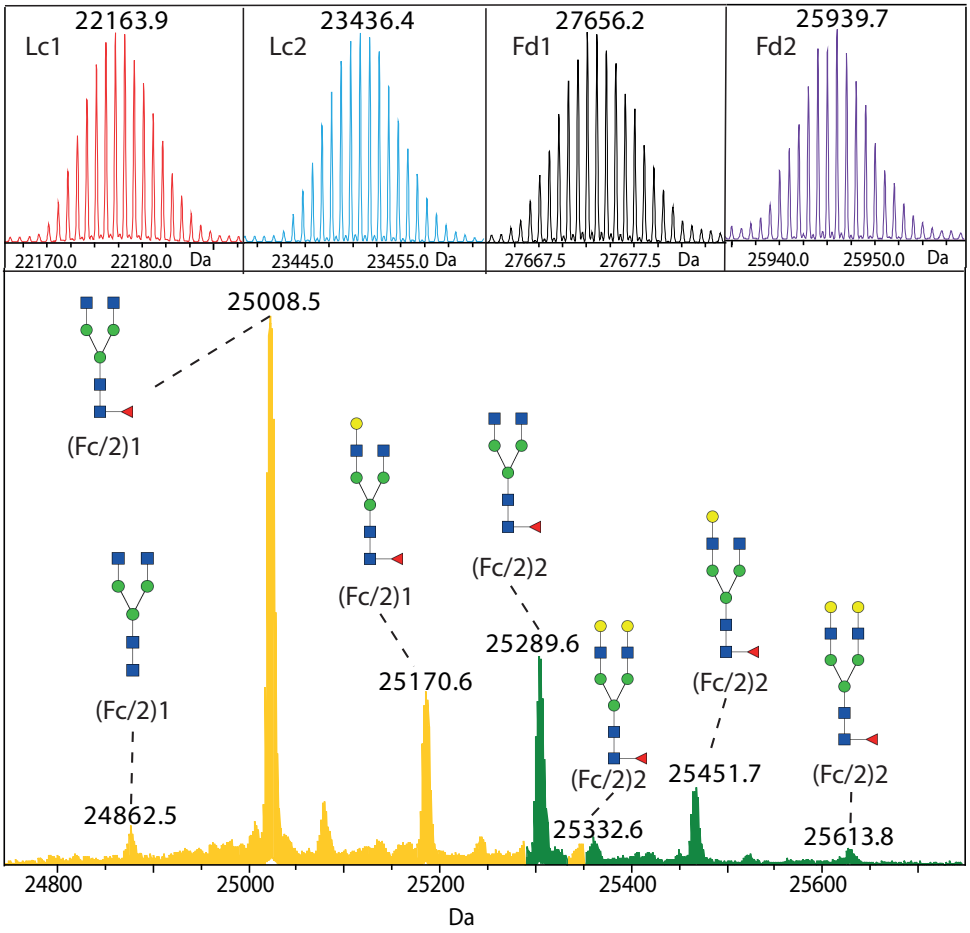

Figure 4. Deconvoluted mass spectra of the Lc1 (red), Lc2 (blue), Fd'1 (black) and Fd'2 (purple) obtained after sheathless CE-FT-ICR-MS of mAb1. Additional Fc/2 fragments ((Fc/2)1 in yellow and (Fc/2)2 in green) are shown with different glycoforms (G0, G0F, G1F, G2F). BGE: 20% Acetic acid containing 10% MeOH.

The same conditions were applied for the analysis of the bispecific BsAb2 obtained after SpeB digestion and reduction (**Figure 5**). Interestingly, the separation profile of these two antibodies was quite different. The migration window of the six subunits of BsAb2 was shorter, only 3.5 min compared to 5 min for BsAb1, and the migration pattern changed. In this case, comigration of Fd'2 and Lc2 was not observed. The alteration in the migration pattern can be explained by the different cleavage site of SpeB together with the exchange of certain amino acids of BsAb2 with respect BsAb1. This change in the primary structure was reflected in a different charge of the analyzed subunits and, therefore, in their electrophoretic mobility (**Tables S2** and **S3**).

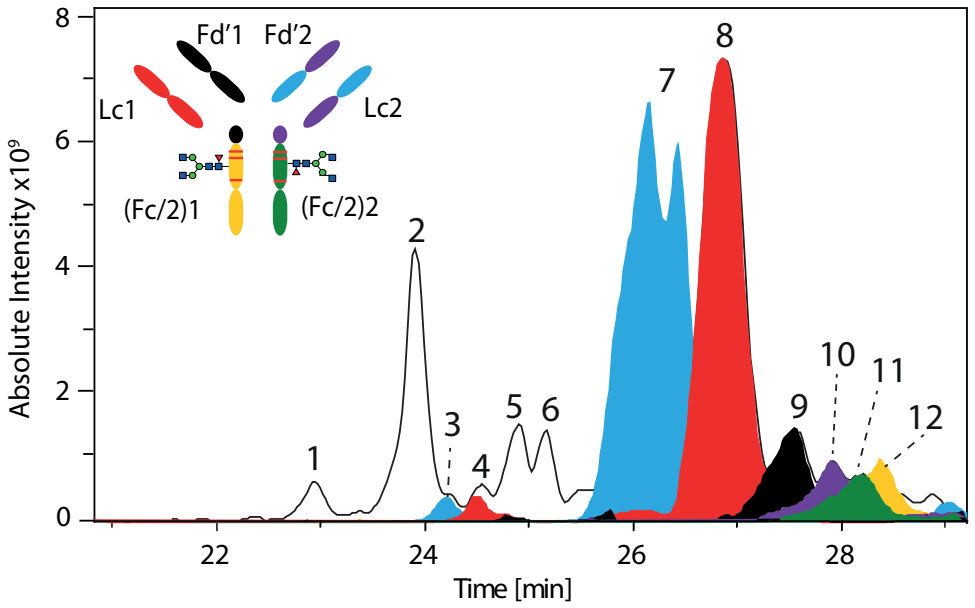

Figure 5. BPE (black trace) and EIEs (color fill) for all the six subunits (7-12, compare Table S4) of BsAb2 obtained by sheathless CE-FT-ICR-MS after SpeB cleavage and DTT reduction. Truncated versions of BsAb2 are numbered from 1-6 (compare Table S5). BGE: 20% Acetic acid containing 10% MeOH. EIEs: Peak 7 (1012.15+1060.11+1113.12±0.1 m/z); Peak 8 (1165.59+1116.86+1171.95±0.1 m/z); Peak 9 (1040.36+998.21+084.97±0.1 m/z); Peak 10 (917.61+950.83+986.08±0.1 m/z); Peak 11 (922.47+956.14+993.47±0.1 m/z); Peak 12 (1004.28+1044.41+967.16±0.1 m/z).

A total of 36 proteoforms including truncated forms could be detected (**Table S4** and **S5**). In this case, Fd'2 was detected with a Pyro-Glu instead of Fd'1. The rest of the subunits did not carry N-terminal glutamine or glutamic acid. For both Lcs a signal with additional +162.05 Da was observed which was assigned to their glycated forms. This modification was not observed at the intact level as the mass shift overlapped with different galactosylation levels of the glycoforms. This illustrates once more the complementarity of both approaches. Furthermore, the Fd's were detected without C-terminal Thr. For Fd'2 also a form without His and Thr was found. These specific truncations have been previously reported and assigned to unspecific cleavages of the enzyme in the hinge region with SpeB[35]. In addition, several truncated versions of Lc1, Lc2 and Fd'1 with masses between 5569.72 Da and 24828.13 Da were detected. These masses were not observed when the intact BsAb2 was analyzed suggesting that they may be the result of unspecific cleavages by endoprotease SpeB. Still, reliable subunit-specific characterization of BsAb2 was possible permitting to assign modifications such as pyro-Glu to specific chains and to determine levels of glycation in the antibody.

6.5 Conclusion

This manuscript shows, for the first time, the potential of sheathless CE-MS for the characterization of BsAbs. A combination of intact and subunit-specific analyses permitted the assessment of their macro- and microheterogeneity. The developed method was successfully applied to characterize two highly homologous BsAbs produced using common engineering techniques. By analyzing the intact antibodies several incomplete assemblies and free chains were detected. The levels of these assemblies were different between the BsAb illustrating that different engineering processes can result in different macroheterogeneity. By performing a subunit-specific analysis, particular PTMs such as glycation could be determined and assigned to each specific subunit. For BsAb1 with an unaltered hinge (compared to conventional mAbs) the well-accepted enzyme IdeS provided effective digestion while for BsAb2 containing the common LALA PG mutation an alternative enzyme, SpeB, permitted the characterization of the antibody subunits. Both, intact BsAbs and BsAb-subunits could be analyzed using a PEI-coated capillary and an acidic BGE showing large applicability. The followed strategy has potential for the characterization of new BsAbs formats of different sizes such as Fab-elongated BsAbs or other Fc fusion protein.

6.6 Supporting information

Supplementary information is available free of charge on the Analytica Chimica Acta website: DOI: 10.1016/j.aca.2020.07.069

6.7 Acknowledgments

This work was supported by the Analytics for Biologics project (Grant agreement ID 765502) of the European Commission and the Netherlands Organization for Scientific Research NWO (SATIN project, Grant No. 731.017.202).

6.8 References

1. Schmid A. S., Neri D. Advances in antibody engineering for rheumatic diseases. Nat Rev Rheumatol 2019, 15, 197-207.
2. Tiller K. E., Tessier P. M., Advances in Antibody Design. Annu Rev Biomed Eng 2015, 17, 191-216.
3. Czajkowsky D. M., *et al.* Fc-fusion proteins: new developments and future perspectives. EMBO Mol Med 2012, 4, 1015-1028.
4. Sedykh S. E., *et al.* Bispecific antibodies: design, therapy, perspectives. Drug Des Dev Ther 2018, 12, 195-208.
5. Knight T., Callaghan M. U. The role of emicizumab, a bispecific factor IXa- and factor

X-directed antibody, for the prevention of bleeding episodes in patients with hemophilia A. Ther Adv Hematol 2018, 9, 319-334.
6. Brinkmann U., Kontermann R. E. The making of bispecific antibodies. MAbs 2017, 9, 182-212.
7. Klein C., Schaefer W., Regula J. T. The use of CrossMAb technology for the generation of bi- and multispecific antibodies. MAbs 2016, 8, 1010-1020.
8. Ignjatovic J., *et al.* Aggregation of Recombinant Monoclonal Antibodies and Its Role in Potential Immunogenicity. Curr Pharm Biotechnol 2018, 19, 343-356.
9. Abes R., Teillaud J. L. Impact of Glycosylation on Effector Functions of Therapeutic IgG. Pharmaceuticals (Basel), 2010, 3, 146-157.
10. Wang W. R., *et al.* Impact of methionine oxidation in human IgG1 Fc on serum half-life of monoclonal antibodies. Mol Immunol 2011, 48, 860-866.
11. Wei Z. P., *et al.* Identification of a single tryptophan residue as critical for binding activity in a humanized monoclonal antibody against respiratory syncytial virus. Anal Chem 2007, 79, 2797-2805.
12. Zhang H., Cui W. D., Gross M. L. Mass spectrometry for the biophysical characterization of therapeutic monoclonal antibodies. Febs Lett 2014, 588, 308-317.
13. Haberger M., *et al.* Rapid characterization of biotherapeutic proteins by size-exclusion chromatography coupled to native mass spectrometry. MAbs 2016, 8, 331-339.
14. Duivelshof B. L., *et al.* A generic workflow for the characterization of therapeutic monoclonal antibodies—application to daratumumab. Anal and Bioanal Chem 2019, 411, 4615-4627.
15. Tassi M., *et al.* Advances in native high-performance liquid chromatography and intact mass spectrometry for the characterization of biopharmaceutical products. J Sep Sci 2018, 41, 125-144.
16. Camperi J., Pichon V., Delaunay N. Separation methods hyphenated to mass spectrometry for the characterization of the protein glycosylation at the intact level. J Pharm Biomed Anal 2020, 178, 112921.
17. Resemann A., *et al.* Full validation of therapeutic antibody sequences by middle-up mass measurements and middle-down protein sequencing. MAbs 2016, 8, 318-330.
18. Turner A., *et al.* Development of orthogonal NISTmAb size heterogeneity control methods. Anal and Bioanal Chem 2018, 410, 2095-2110.
19. Woods R. J., *et al.* LC-MS characterization and purity assessment of a prototype bispecific antibody. MAbs 2013, 5, 711-722.
20. Liu H., Gaza-Bulseco G., Chumsae C. Analysis of Reduced Monoclonal Antibodies Using Size Exclusion Chromatography Coupled with Mass Spectrometry. J Am Soc Mass Spectrom 2009, 20, 2258-2264.
21. Ding W., *et al.* Improving Mass Spectral Quality of Monoclonal Antibody Middle-Up LC-MS Analysis by Shifting the Protein Charge State Distribution. Anal Chem 2018, 90, 1560-1565.

22. Sokolowska I., *et al.* Subunit mass analysis for monitoring antibody oxidation. MAbs 2017, 9, 498-505.
23. Wang C., *et al.* A systematic approach for analysis and characterization of mispairing in bispecific antibodies with asymmetric architecture. MAbs 2018, 10, 1226-1235.
24. D'Atri V., *et al.* Hydrophilic Interaction Chromatography Hyphenated with Mass Spectrometry: A Powerful Analytical Tool for the Comparison of Originator and Biosimilar Therapeutic Monoclonal Antibodies at the Middle-up Level of Analysis. Anal Chem 2017, 89, 2086-2092.
25. Belov A. M., *et al.* Complementary middle-down and intact monoclonal antibody proteoform characterization by capillary zone electrophoresis - mass spectrometry. Electrophoresis 2018, 39, 2069-2082.
26. Haselberg R., *et al.* Heterogeneity assessment of antibody-derived therapeutics at the intact and middle-up level by low-flow sheathless capillary electrophoresis-mass spectrometry. Anal Chim Acta 2018, 1044, 181-190.
27. Giorgetti J., *et al.* Intact monoclonal antibodies separation and analysis by sheathless capillary electrophoresis-mass spectrometry. Eur J Mass Spectrom 2019, 25, 324-332.
28. Chen C. H., *et al.* Intact NIST monoclonal antibody characterization-Proteoforms, glycoforms-Using CE-MS and CE-LIF. Cogent Chem, 2018, 4, 1480455.
29. Giorgetti J., *et al.* Combination of intact, middle-up and bottom-up levels to characterize 7 therapeutic monoclonal antibodies by capillary electrophoresis - Mass spectrometry. J Pharm Biomed Anal, 2020, 182, 113107.
30. Marcia R Santos C. K. R., Fonslow B., Guttman A. A covalent, cationic polymer coating method for the CESI-MS analysis of intact proteins and polypeptides. 2015.
31. Schlothauer T., *et al.* Novel human IgG1 and IgG4 Fc-engineered antibodies with completely abolished immune effector functions. Protein Eng Des Sel 2016, 29, 457-466.
32. Michalikova K., *et al.* Middle-Up Characterization of the Monoclonal Antibody Infliximab by Capillary Zone Electrophoresis-Mass Spectrometry. Lc Gc Europe 2019, 32, 130-137.
33. Faid V., *et al.* Middle-up analysis of monoclonal antibodies after combined IgdE and IdeS hinge proteolysis: Investigation of free sulfhydryls. J Pharm Biomed Anal 2018, 149, 541-546.
34. Gstottner C., *et al.* Monitoring glycation levels of a bispecific monoclonal antibody at subunit level by ultrahigh-resolution MALDI FT-ICR mass spectrometry. MAbs 2020, 12, 1682403.
35. Lippold S., *et al.* Proteoform-Resolved FcγRIIIa Binding Assay for Fab Glycosylated Monoclonal Antibodies Achieved by Affinity Chromatography Mass Spectrometry of Fc Moieties. Front Chem 2019, 7.